

Edges Extraction Method based on Fractal and Wavelet

Qingsheng Zhu

College of Computer Science, Chongqing University, Chongqing, China
qs Zhu@cqu.edu.cn

Yanxia Wang

College of Computer Science, Chongqing University, Chongqing, China
cloudwyx@163.com, lhjclr@cqu.edu.cn

Huijun Liu

College of Computer Science, Chongqing University, Chongqing, China
cloudwyx@163.com, lhjclr@cqu.edu.cn

Abstract—The paper presents a method combining fractal with wavelet for edges extraction. We firstly compute fractal dimension values of R, G, B components of every pixel in image, and synthesize color image by normalized fractal dimension values. Then we decompose histogram of synthetic image by wavelet transform to determine the threshold of extraction edges, at the same time, improve the thresholding segmentation based on wavelet transform – AEEM (Automatic Extraction Edges Method) which determines automatically the threshold. Our experimental results demonstrate that the approach can gain better segmentation than histogram-based approach.

Index Terms— Wavelet Decomposition, Multi-resolution Analysis, Fractal, Box-counting Dimension.

I. INTRODUCTION

Image segmentation is a key pre-processing step in area of image analysis and image understanding^[1]. It is broadly applied in image recognition, image compression, image retrieval, and computer vision^[2-4]. In many applications, the quality of final object classification and scene interpretation depends on the quality of segmented output. The goal of segmentation is to identify homogenous regions according to pixel characteristics and correlation among adjacent pixels in order to achieve the feature extraction and recognition of the objects in images^[5]. In the process of feature extraction and recognition, edges are one of the most merchant descriptors of image content, they define the shapes of objects. There are many image segmentation techniques, which can be classified into histogram-based, edge-based, region-based, clustering and combination of these techniques^[6].

A widely used technique for image processing is the histogram-based threshold, which assumes that images are composed of regions with different gray level ranges, the histogram of an image can be separated into a number of peaks, each corresponds to a region, and the valleys between any two adjacent peaks corresponds to

edges. The gray histogram often combines gray value distribution map to determine the threshold for extraction edge. The advantages of gray histogram are that it does not need a priori information of image and has a simple calculation. But the histogram-based technique do not consider spatial relationship of pixels. To overcome this drawback, this paper makes use of fractal and wavelet to extract edges.

Fractal geometry is a powerful tool to describe and to process anomalous graphics. There are many literatures on fractal geometry in image retrieval, image compression and image segmentation. The quantitative parameter to describe fractal character is fractal dimension which reflects regularity and complexity of distribution of image texture and gray. Edges of objects in images have fractal character in particular images about natural-scene. Objects with different fractal feature have different fractal dimension, which is a basic character for image segmentation and feature extraction.

The paper makes use of relativity among adjacent pixels and gray distribution characteristics to compute fractal dimension of each pixel. As the fractal dimension of image pixels is smaller for the whole image, its change frequency is larger. The wavelet analysis has local analysis and detailed function, and can reveal signal trend as well as self-similarity. Therefore, the paper presents the idea that fractal is combined with wavelet to extract edges. The edges of objects in image are extracted by wavelet decomposing the histogram of fractal dimension values synthetic image to determine automatically threshold by wavelet coefficients.

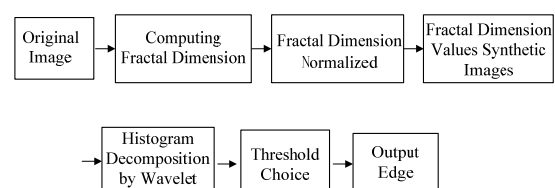


Fig.1. Flowchart of Edge Extraction

In section 2, we present box-counting dimension concept and calculation. The method of fractal dimension normalized and the multi-resolution analysis based on 2-band for 1D signal. In Section 3, our experiments and analysis are shown.

II. EDGE EXTRACTION APPROACH

Fractal geometry is a theory for studying non-linear complex systems. Fractal, characterized by self-similar structure, is proposed by Mandelbrot^[7] in 1982. The self-similar feature means that, irrespective of shape complexity of an object, an observer can find the similar shapes on contractible scales by looking into its structure. Pentland presented evidence that most natural surfaces are spatially isotropic fractals and the intensity images of these surfaces are also fractals^[8].

The surface roughness was characterized through a fractal technique quantified by a non-dimensional number called the fractal dimension^[7]. It offers the potential of unifying and simplifying various two dimensional texture descriptions, as well as the possibility of interpreting them in terms of three dimensional structure of the image. For digital images, the surface roughness is different, in homogeneous color region, the surfaces are smoother correspondingly, and that edges of between background and objects are rougher. So their fractal dimensions are also different. In this paper, a large number of experiments show that the fractal dimension values of an image are most between 1 and 2. And it measures the degree of irregularity and roughness of the grey level surface in a 3D space; the more the color is consistent (respectively, rough), the more its fractal dimension is near 1(respectively, 2). For the whole image, the change frequency of fractal dimension is larger. As wavelet analysis has the local analysis and detailed function, and can reveal the signal trend as well as self-similarity, and so on. Therefore, the paper makes use of wavelet to analyze the histogram of fractal dimension, and extract the edges of objects according to wavelet coefficients to choose the threshold. Flowchart is shown as Fig.1.

A. Measurement of Fractal Dimension

A important parameters in fractal analysis is fractal dimension D , which increases with increase of structure complexity describing self-similar structure and degree of irregular of fractal objects. Fractal geometry involves various approaches to define fractional dimension, the most common of which is Hausdorff's dimension, also known as the similarity dimension^[9].

Let a non-empty and bounded set, F , in Euclidean n -space be self-similar, if F is the union of $N_\delta(F)$ nonoverlapping copies of itself scaled down by a ratio, δ , in all coordinates from the whole. The Hausdorff's dimension (fractal dimension) of a non-empty and bounded set, F , in R^n is a real number used to characterize the geometrical complexity of F . The fractal dimension D_f of F can be derived from the relation^[10]

$$D_f = \lim_{\delta \rightarrow 0} \frac{\log N_\delta(F)}{-\log \delta} \tag{1}$$

While the definition of fractal dimension via self-similarity is straightforward, it is difficult to compute directly from the image data. However, a related measure of fractal dimension can be computed from a fractal set, F , in R^n . Several approaches exist to estimate fractal dimension in an image. One of the commonly used methods proposed by Chaudhuri and Sarkar^[11] is based on the differential box-counting (DBC) algorithm^[12]. Instead of directly measuring an image surface, the measures at different scales are obtained by means of counting the minimum number of boxes of different size, which can entirely cover the whole surface. Taking account that obtaining the optimal box number usually involves complex optimization, this method adopts the regular partition scheme to gain an approximation of $N_\delta(F)$. The process can be detailed as follows.

For a given integer s , an $M \times M$ image is portioned into grids of size $s \times s$ where $1 < s \leq M/2$. Then the scale radio δ becomes s/M . On each grid, there is a column of $s \times s \times s'$ boxes. If the maximum gray level is G , then $\left[\frac{G}{s'} \right] = \left[\frac{M}{s} \right]$. The image is viewed as a three-dimensional (3-D) surface, where denotes the 2-D position and the third coordinate denotes the gray level of the corresponding pixel. Let the minimum and maximum gray level of the image in the $(i, j)^{th}$ grid fall in the k^{th} and the l^{th} boxes, respectively. The number of boxes needed to cover the image surface on that grid is calculated as

$$n_\delta(i, j) = l - k + 1 \tag{2}$$

and the total number of boxes needed to cover the whole surface can then be approximately estimated as follows:

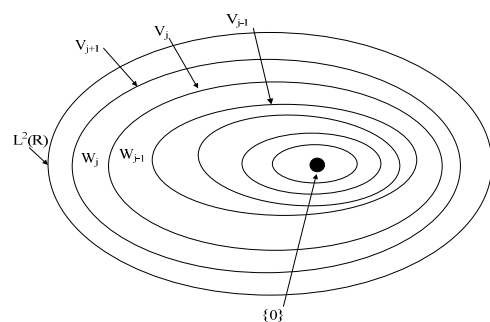


Figure 2. Decomposition of $L^2(R)$

$$N_\delta = \sum_{i,j} n_\delta(i, j) \tag{3}$$

Where N_δ is counted for different values for δ (i.e. different values of s). Then using (1) we can estimate D , the fractal dimension, from the least squares linear fit of

$\log N_\delta$ against $\log \frac{1}{\delta}$. In the actual implementation, a random placement of boxes is applied in order to reduce quantization effects.

B. Fractal Dimension Normalized

Fractal provides a proper mathematical framework to study the irregular and complex shapes that exist in nature. Hence, if the pixel intensity of digital images is regarded as the height above a plane then the intensity surface can be viewed as a rugged surface. Researchers have proved that the surface roughness has fractal characteristics^[13]. The FD could reflect the surface complexity. The smooth region has identical or approximate fractal dimensions, in the same way, there are identical or approximate fractal dimensions for rough surface. So the homogeneous color region and edges between objects has different fractal dimensions. For there are obvious textures of the image which is synthesized by the fractal dimension values of pixels in R,G, B color space, we normalize the fractal dimension, the formula as follow

$$D_n = T(D/D_{max}) \tag{4}$$

Where D and D_{max} is the fractal dimension value of pixels and the largest fractal dimension value, respectively; n denotes the number of pixels. The function $T(d)$ satisfies the following conditions.

- 1) The function $T(d)$ is the single-valued and monotonically increasing in the interval $[0,1]$;
- 2) When $d \in [0,1]$, then $0 \leq T(d) \leq 1$.

C. Multi-resolution Analysis

Multiresolution analysis permits the decomposition of a signal into numerous detailed signals and approximate signals at various resolutions where each resolution characterizes distinct physical structures within the signal. The formulation represents a signal by decomposing it into subbands and each subband can then be treated individually based on its characteristic.

An $L^2(R)$ multiresolution analysis(as Fig.2.)^[14] consists of closed, nested approximation spaces V_j and a scaling function ϕ which satisfy the following properties for any $f \in L^2(R)$ ^[15].

- 1) $\dots V_{-2} \subset V_{-1} \subset V_0 \subset V_1 \subset V_2 \subset \dots$
- 2) $\bigcup_{j \in \mathbb{Z}} V_j = L^2(R)$; $\bigcap_{j \in \mathbb{Z}} V_j = \{0\}$
- 3) $f(x) \in V_j \Leftrightarrow f(2x) \in V_{j+1}$; $j \in \mathbb{Z}$
 $f(x) \in V_j \Rightarrow f(x + \frac{n}{2^j}) \in V_j$; $n \in \mathbb{Z}$

The set of functions $\{2^{j/2} \phi(2^j x - n) \mid n \in \mathbb{Z}\}$ forms an orthonormal basis for the approximation space V_j .

The projection of an $L^2(R)$ function $f(x)$ on V_j is the j th resolution approximation of $f(x)$, denoted by $f_j(x)$. Then

$$f_j(x) = \sum_{n \in \mathbb{Z}} a_{jn} 2^{j/2} \phi(2^j x - n)$$

$$a_{jn} = \langle f, \phi_{jn} \rangle = \int_{-\infty}^{\infty} f(x) 2^{j/2} \phi(2^j x - n) dx \tag{5}$$

With a_{jn} representing the j th approximation coefficient and $\langle \bullet \rangle$ denotes the inner product, $\phi_{jn} = 2^{j/2} \phi(2^j x - n)$ is called a scaling function.

Because of property 1), $f_j(x) \rightarrow f(x)$ in $L^2(R)$ as $j \rightarrow \infty$ and formula (5) provides a multiresolution approximation $f(x)$. In some occasions it is preferable to decompose $f(x)$ in orthogonal subspaces, rather than nested ones. Mallat^[16] has shown one can create a mother wavelet $\varphi(x)$ such that the set of functions $\{2^{j/2} \varphi(2^j x - n) \mid n \in \mathbb{Z}\}$ forms an orthonormal basis for W_j . The spaces W_j , where $j \in \mathbb{Z}$, are mutually orthogonal, and provide an orthogonal decomposition of V_j into 2 subspaces, namely

$$V_{j+1} = V_j \oplus W_j \tag{6}$$

W_j is typically referred to as the j th detail space, because it captures the difference in signal information between the approximation spaces V_{j+1} and V_j .

The projection of $f(x)$ on W_j is the j th detail signal

$$f_j(x) = \sum_{n \in \mathbb{Z}} d_{jn} 2^{j/2} \varphi_{jn}(2^j x - n)$$

$$d_{jn} = \langle f, \varphi_{jn} \rangle = \int_{-\infty}^{\infty} f(x) 2^{j/2} \varphi_{jn}(2^j x - n) dx \tag{7}$$

With d_{jn} representing the j th detail coefficient and $\langle \bullet \rangle$ denotes the inner product. The scaling functions and the mother wavelet are related by the ‘‘two-scale’’ recursion relations

$$\phi(x) = \sum_{n=-\infty}^{\infty} h_n \sqrt{2} \phi(2x - n)$$

$$\varphi(x) = \sum_{n=-\infty}^{\infty} g_n \sqrt{2} \phi(2x - n) \tag{8}$$

Where h_n and g_n denote scaling and wavelet filters, respectively. $\phi(x)$ and $\varphi(x)$ are mutually orthogonal functions. Formula (5), (7), (8) show that approximation and detail signals can be computed by convolving a_{jn} with the filter h_n and d_{jn} with the filter g_n respectively and retaining every other sample of the output. That is to say, the coefficients of the $j + 1$ st approximation level are

simultaneously decomposed into the j th detail and approximation coefficients using the low-pass and high-pass impulse responses $h(n)$ and $g(n)$. The 1D signal multiresolution analysis is illustrated by the block diagram shown in Fig.3. Any dimension can be extended from the 1D.

The input signals f is projected onto the appropriate approximation or detail space to create approximation and detail signals. Since each space is spanned by an orthonormal basis set, the signal projection onto a given approximation or detail space at the j th resolution is equivalent to the sequence of projection coefficients.

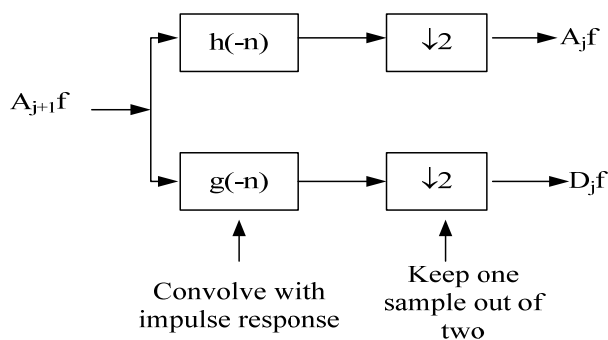


Fig.3. 1D subband transform for decomposition of a discrete approximation A_{j+1} into an approximation at a coarser resolution A_j and the signal detail D_j

III. EXPERIMENTAL AND ANALYSIS

A. Choice of Sliding Window Size

Fractal texture needs to compute fractal dimension of every pixel in image, the paper takes fractal dimension value computed by sliding window as the fractal dimension value of the central point in sliding window. Therefore, the choice of sliding window size is very important, when window is too small, the fractal dimension can represent well edges of gray drastic change, and not manifest precisely texture characteristics because measure values of homogeneous textures change large; Window is too large, homogeneous textures can be expressed precisely, but edges are bad distortion, and with the larger window, the calculation also increases rapidly. In order to manifest better homogeneous textures and edges, we make experiments to confirm that the size 3×3 or 5×5 of the sliding window is more appropriate. The image (Fig.4 (a)) is the synthetic picture by drawing board, the fractal dimension of every pixel is computed by the size 3×3 , 5×5 , 7×7 and 9×9 window respectively, and then extracting edges according to fractal dimension, the effect of a variety of sliding windows can be seen from the following figure. The edges and textures have better results for 3×3 and 5×5 window, but edges are bad distortion for 7×7 and 9×9 window. The size 5×5 window is used in experiments.

The extraction process is divided into two main stages. In the first stage, the fractal demission of the R, G and B components of image are respectively computed in RGB

color space, each color component is considered in a three-dimensional (3D) space, represented by the position of the pixel and its intensity $(i, j, f(i, j))$, at each pixel (i, j) using sliding grid of size 5×5 pixels around (i, j) . On each grid there is a column of boxes of size $5 \times 5 \times 5$, computing N_s and fractal dimension values of each color component respectively according to formulas (3), (1), then normalized fractal dimension by the formula (4). In order to choose automatically the threshold, the normalized fractal dimensions of the R, G and B color components synthesize the color image using the function of synthetic color image in Matlab7.0.

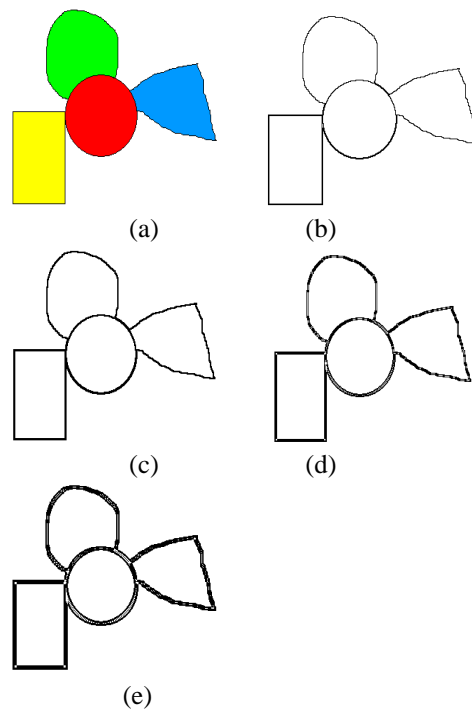


Fig.4 (a)Original picture, (b)Extraction Edge by the Size 3×3 Window, (c)Extraction Edge by the Size 5×5 Window, (d) Extraction Edge by the Size 7×7 Window, (e)Extraction Edge by the Size 9×9 Window

B. Extraction of edges

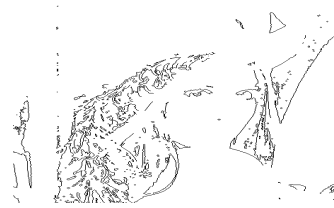
In the second stage, firstly, it computes the histogram of original images and synthetic images of the normalized fractal dimension values. We determine the peaks and valleys and apply threshold to the images. Selection of correct peaks and thresholds are important for achieving good results. The threshold is determined by the peaks of histogram and the valleys of gray change rate distribution map for original images. For the synthetic image, the paper uses the Automatic Extraction Edges Method which is improved thresholding segmentation method of based on wavelet transform to determine extraction threshold. The basic idea of the algorithm is that the histogram curve is decomposed multi-resolution by formula (5), determining the extraction threshold according to decomposition coefficient. Steps as following:



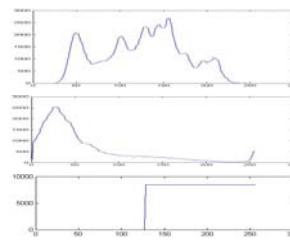
(a)



(b)



(c)

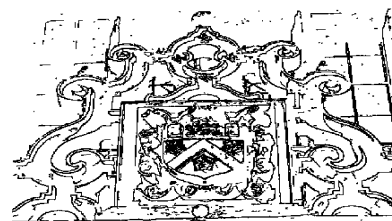


(d)

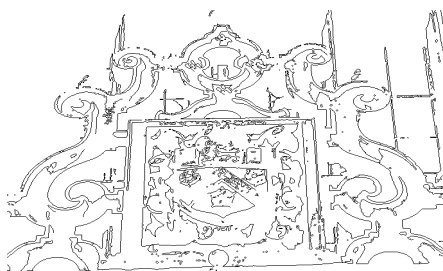
Fig.5 (a) Original image, (b) Fractal-wavelet texture extraction Approach, (c) histogram-based approach, (d) histogram of original image, histogram of synthetic image by fractal dimension values of original image, $j=-7$ wavelet decomposition coefficient from top to bottom respectively



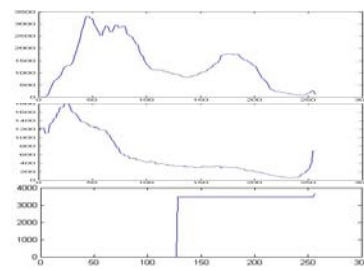
(a)



(b)



(c)

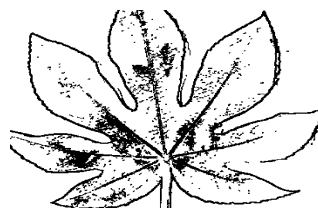


(d)

Fig.6 (a) Original image, (b) Fractal-wavelet texture extraction Approach, (c) histogram-based approach, (d) histogram of original image, histogram of synthetic image by fractal dimension values of original image, $j=-6$ wavelet decomposition coefficient from top to bottom respectively



(a)



(b)



Fig.7 (a) Original image, (b) Fractal-wavelet texture extraction Approach , (c) histogram-based approach, (d) histogram of original image, histogram of synthetic image by fractal dimension values of original image, $j=-7$ wavelet decomposition coefficient from top to bottom respectively

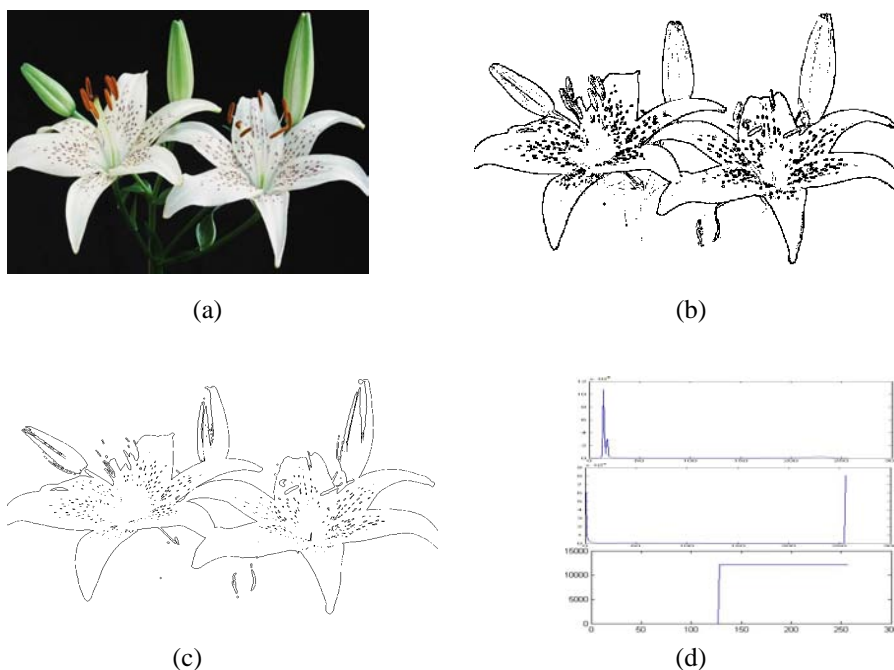


Fig.8 (a) Original image, (b) Fractal-wavelet texture extraction Approach , (c) histogram-based approach, (d) histogram of original image, histogram of synthetic image by fractal dimension values of original image, $j=-5$ wavelet decomposition coefficient from top to bottom respectively

- (a) Let decomposition series $j = -\log_2(L)$, L equals the largest gray in image;
- (b) Compute the histogram h which is smoothed by smooth function;
- (c) Decompose curve h according to formula (5), getting $\{a_k\}_j = \left\{ \left\langle h_f, \varnothing_{j,k} \right\rangle \right\}_{k \in \mathbb{Z}}$;
- (d) Histogram of decomposition coefficient $\{a_k\}_j$, determining the thresholds L_i, L_j , which are the gray values of beginning and ending points of the peak of histogram of decomposition coefficient $\{a_k\}_j$;
- (e) If no peak of histogram of decomposition coefficient $\{a_k\}_j$, then $j = j + 1$, while $j < 0$, skipping (c)
- (f) Comparing pixels gray l with L_i, L_j , pixels gray $L_i \leq l \leq L_j$ are edges or area.

C. Experimental results

To verify the effect of the method the paper presents, comparing with gray histogram threshold method. The experiments are performed on over 50 images collected from the Internet and other sources. Fig.5 illustrates some of the results. Figs.4 (a) is the original images and Figs.4 (b) and (c) are the extraction results respectively by the fractal and wavelet idea and gray histogram-based method. From the results, we observe that the edges of regions in the images are well extracted, all the important details in the images are preserved in Fig.5 (b), For example, the edge of the cap, eyes and noses are clearly visible in the extracted image. In Fig.5 (c), the important details are lost, such as the edge of the cap, noses and mouth. The histogram of original image, histogram of synthetic image and wavelet decomposition coefficient of the histogram of synthetic image are shown in the graphs of Fig.5 (d) top, middle and bottom, respectively.

The Fig.6 shows that histogram-based approach and the approach presented in the paper are similar, all the

important details in the images are preserved. But for the leaf, the main venations are extracted by the approach presented in the paper; histogram-based approach can only extract edges of leaf. From the Fig.8, we observe that the edges of flowers are well extracted, whereas details in the images are preserved in Fig. 8(b) better than in Fig.8(c).

D. The time complexity of algorithm

The computation time is mainly dependent on the size of image. The computational complexity of the proposed algorithm is analyzed as follows. The extraction process consists of two main stages. In the first stage, the fractal dimension values are computed. To compute the fractal dimension value of every pixel, segmenting window $\log_2 s$ times, and the minimum and maximum gray level in every grid must be found, which needs to compare $s \times s$ (s is the size of sliding window) times, so that, the complexity of the first stage is about $O(s \times s \times \log_2 s \times n)$, where n is the total number of pixels, s equals to 5 in the paper. The next step is to determine threshold, it takes most time to compute histogram of images, which is the total number of pixels n . Therefore, the total computational complexity of the proposed algorithm is $O((s \times s \times \log_2 s + 1) \times n)$, the conventional histogram based thresholding algorithm is $O(n)$. As s is smaller, a time complexity of the proposed algorithm and the conventional histogram based thresholding algorithm is the polynomial.

IV. CONCLUSION

The paper has presented a fractal combining with wavelet idea for edges extraction and improved the thresholding segmentation based on wavelet transform, which determines automatically the extraction threshold. The computational complexity of the proposed method is slightly more than the conventional histogram-based thresholding algorithm, but the key point of our approach is that, using wavelet decomposition for selection of threshold results in more realistic values and thus achieves better extraction results. The experimental results show the superiority of the algorithm. The proposed approach may have many image processing applications. Nonetheless, the paper does not give how automatically determine the size of sliding window according to image feature that is the subject in my future work.

ACKNOWLEDGMENT

The authors was supported in part by the National 863 Plan Project of China (No. 2006AA10Z233) and the National Natural Science Foundation of China (No 60773082).

REFERENCES

- [1] Cheng, H.D., Jiang, X.H., Sun, Y., Wang, J. Color image segmentation: Advances and prospects. *Pattern Recognition* 34, 2259–2281, 2001.
- [2] K. Belloulata, J. Konrad, Fractal image compression with region-based functionality, *IEEE Trans. Image Process.* 11 (4), 351–362, 2002.
- [3] Y. Chen, J.Z. Wang, A region-based fuzzy feature matching approach to content-based image retrieval, *IEEE Trans. Pattern Anal. Machine Intell.* 24 (9), 1252–1267, 2002.
- [4] S.L. Hartmann, R.L. Galloway, Depth-buffer targeting for spatially accurate 3-D visualization of medical images, *IEEE Trans. Medical Imaging* 19 (10), 1024–1031, 2000.
- [5] Choi H. Baraniuk R.G.. Multiscale image segmentation using wavelet-domain hidden Markov models[J], *IEEE Trans, Image Proc.*,10(9):1309~1321,2001.
- [6] Aghbari, Z.A., Al-Haj, R.. Hill-manipulation: An effective algorithm for color image segmentation. *Image Vision Compute.* 24 (8), 894–903, 2006.
- [7] B. B. Mandelbrot, *The fractal geometry of nature*, W. H Freeman, New York, 1982.
- [8] A. P. Pentland. Fractal based description of natural scenes. *IEEE Trans. Pattern. Anal. Mach. Intell.*, vol. PAMI-6, no. 6, pp. 661–674, Jun. 1984.
- [9] M.R. Schroeder, *Fractals, Chaos, Power Laws: Minutes from an Infinite Paradise*, W.H. Freeman, New York, 1991.
- [10] Wen-Li Lee, Yung-Chang Chen, Kai-Sheng Hsieh. Ultrasonic Liver Tissues Classification by Fractal Feature Vector Based on M-Band Wavelet Transform. *IEEE Transactions on Medical Imaging*, Vol.22,No.3, March,2003.
- [11] B.B. Chaudhuri and N. Sarkar. Texture segmentation using fractal dimension. *IEEE Trans. Pattern Anal. Mach. Intell.*, vol. 17, no. 1, pp. 72–77, Jan. 1995.
- [12] N. Sarkar and B. B. Chaudhuri. An efficient differential box-counting approach to compute fractal dimension of image. *IEEE Trans. Syst.,Man, Cybern.*, vol. 24, pp. 115–120, Jan. 1994.
- [13] R. Sarathi, R.K. Sahu, T. Tanaka. Understanding the Hydrophobic Characteristics of Epoxy Nanocomposites Using Wavelets and Fractal Technique. *IEEE Transactions on Dielectrics and Electrical Insulation* Vol. 15, No. 1; February 2008.
- [14] Michail K.Tsatsanis, Georgios B. Giannakis. Principal Component Filter Banks for Optimal Multiresolution Analysis. *IEEE Transactions on Signal Processing*, Vol.43,No.8, August 1995.
- [15] Thomas J. Burns, Steven K. Rogers, Mark E. Oxley, A Wavelet Multiresolution Analysis for Spatio-Temporal Signals. *IEEE Transactions on Aerospace and Electronic Systems*, Vol. 32, No. 2, April 1996.
- [16] S. Mallat. A theory for multiresolution signal decomposition: The wavelet representation. *IEEE Trans. Pattern Anal. Machine Intell.*, vol.11,674–693,July 1989.

Qingsheng Zhu, Professor, tutor of a Ph.D. student, College of Computer Science, Chongqing University, Chongqing, China.

Huijun Liu, Ph.D. student, College of Computer Science, Chongqing University, Chongqing, China.

Yanxia Wang, Ph.D. student, College of Computer Science, Chongqing University, Chongqing, China.